Electronic Supplementary Material (ESI) for Journal of Materials Chemistry A.

Indirect-to-Direct Bandgap Transition in Layered Metal Halide Perovskite - $CsPb_2Br_5$

–Electronic Supplementary Information

Xiao Wu,[a] Xiangyu Zhang,[a, b] Wei Yu,[a] Yongxiang Zhou, [a, b] Walter Wong, [a] Weixin He, [a] Kian Ping Loh,[a] Xiao-Fang Jiang,*[c] and Qing-Hua Xu*[ab]

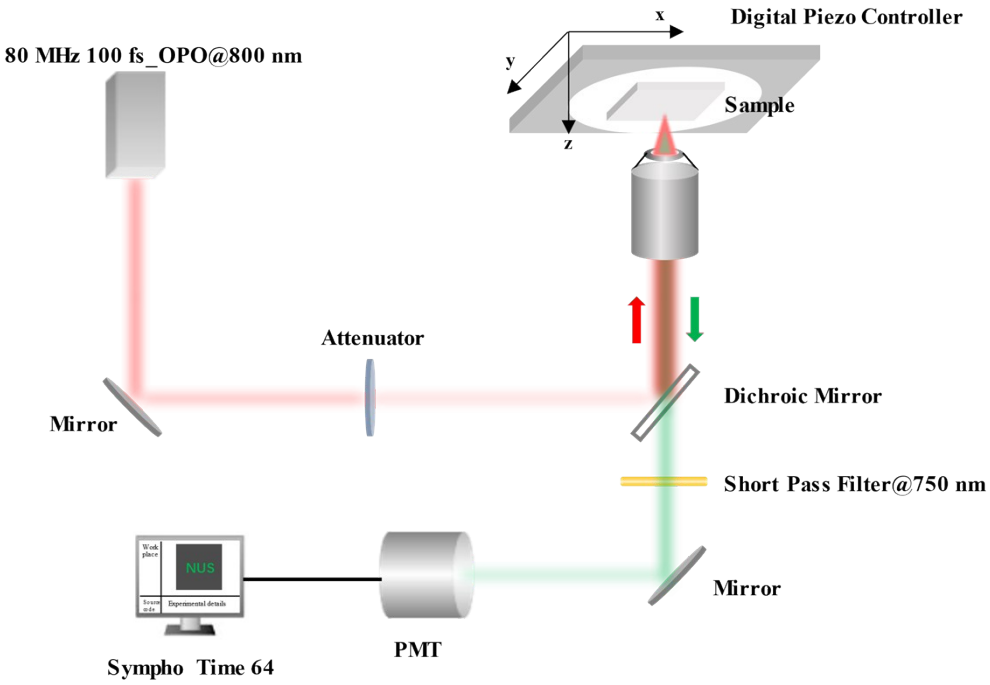

Figure S1 Schematic diagram of the optical system for laser writing and reading.

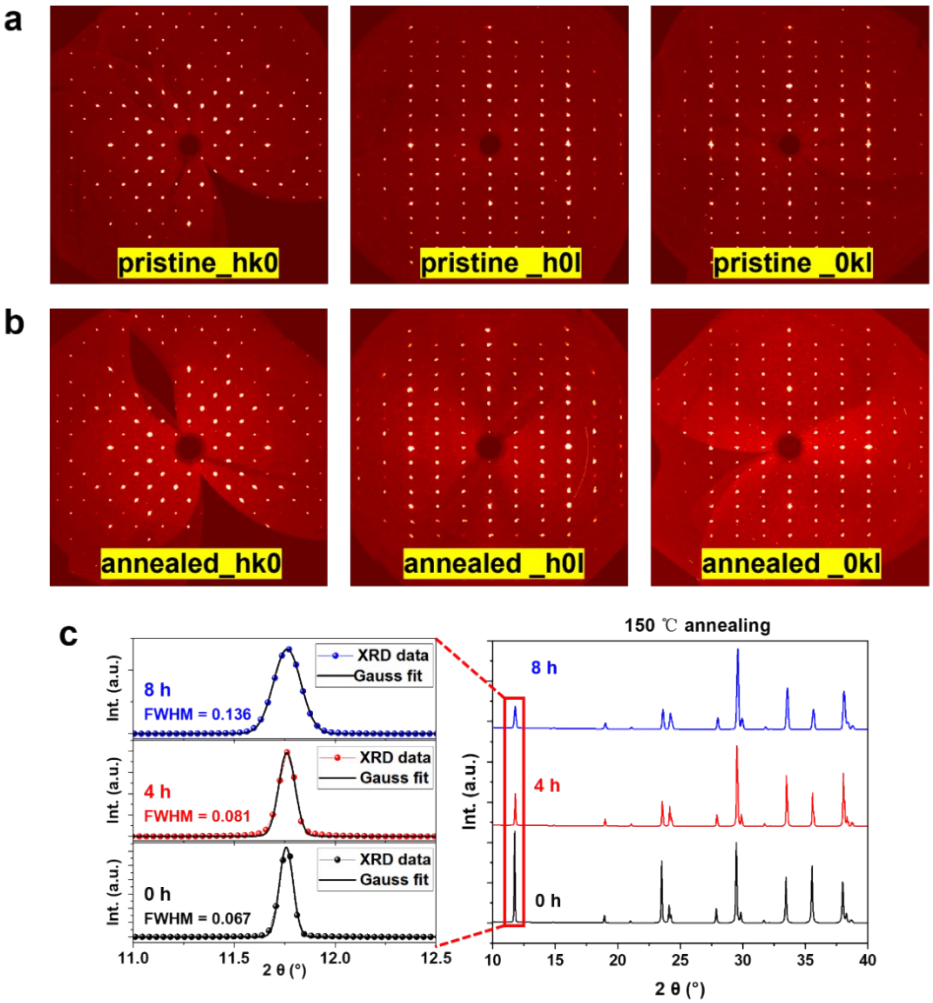

Figure S2 (**a**) Precession images derived from single crystal X-ray diffraction patterns of the pristine $CsPb_2Br_5$ SCs and (**b**) annealed $CsPb_2Br_5$ SCs (150 ℃, 8 h); (**c**) Powder-XRD of $CsPb_2Br_5$ SC-powder with annealing time of 0/4/8 h at 150 ℃.

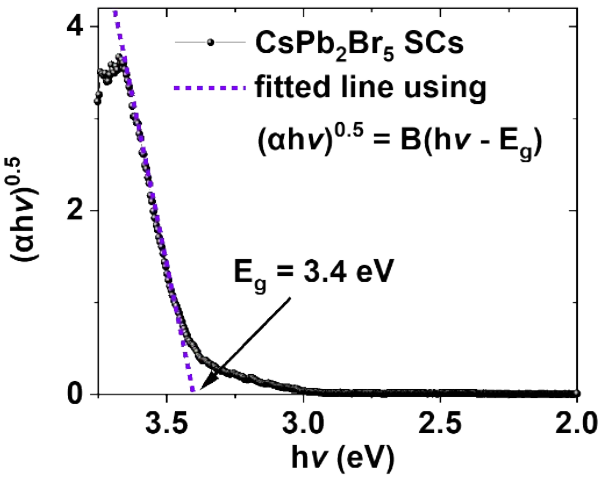

Figure S3 Indirect bandgap of $CsPb_2Br_5$ SCs obtained by using the Tauc method.

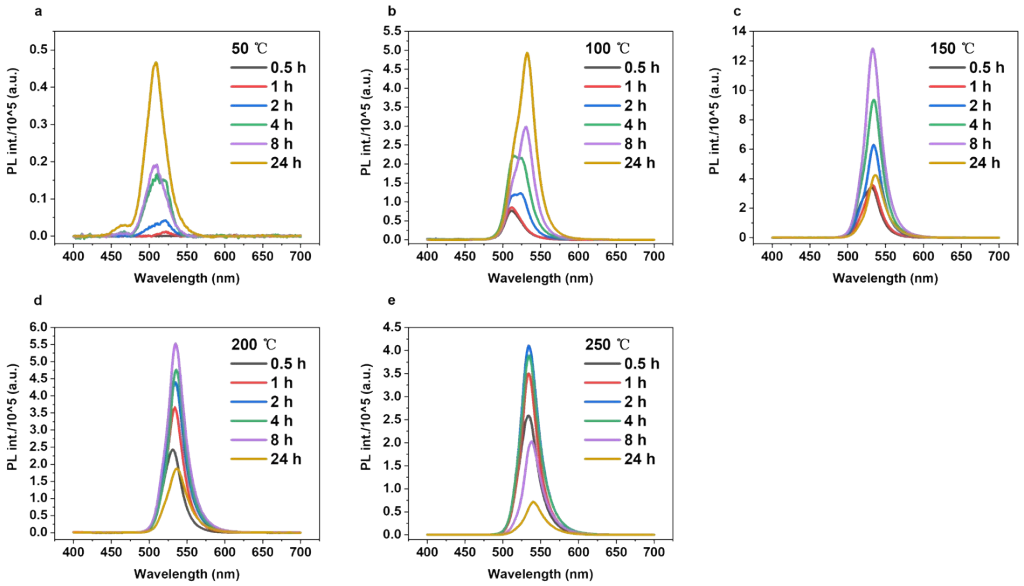

Figure S4 PL spectra of $CsPb_2Br_5$ SCs under thermal annealing at different temperatures for different time periods.

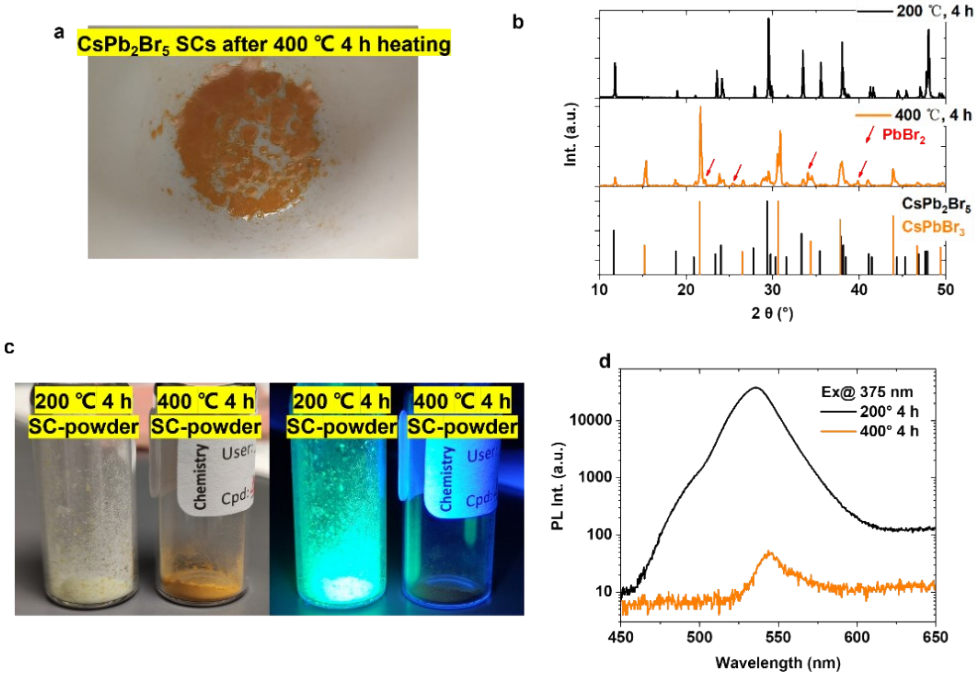

Figure S5 (**a**) Photograph of $CsPb_2Br_5$ SCs after thermal annealing at 400 °C for 4 hrs. (**b**) Powder-XRD patterns of $CsPb_2Br_5$ SCs after thermal annealing at 200/400 °C for 4 hrs and the comparison with JCPDS card of $CsPb_2Br_5$ (25-0211) and $CsPbBr_3$ (54-0752). (**c**) Photograph of $CsPb_2Br_5$ SC-powder after thermal annealing at 200/400 °C for 4 hrs under daylight and UV light. (**d**) PL spectra of $CsPb_2Br_5$ SC-powder after thermal annealing at 200/400 °C for 4 hrs.

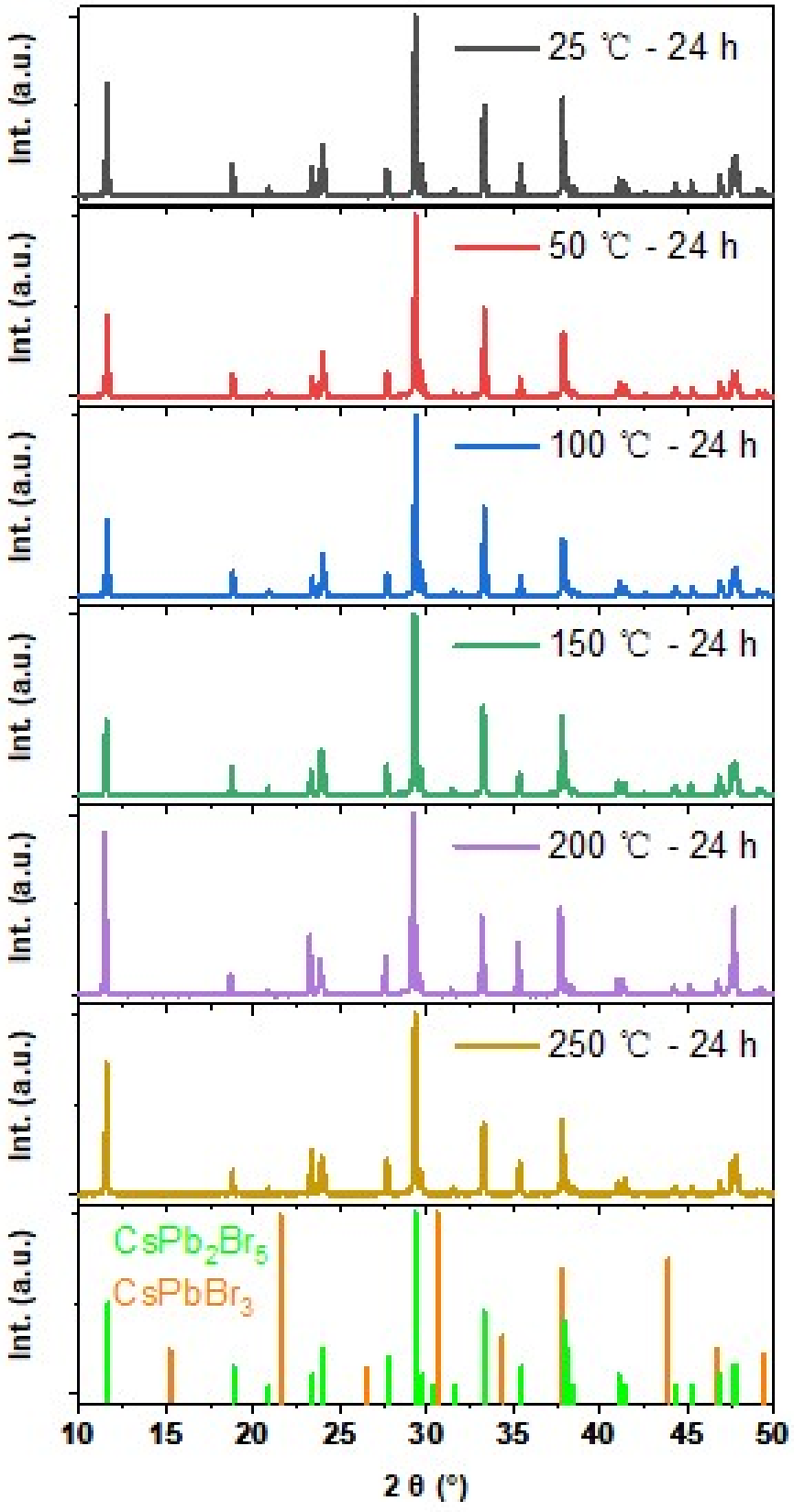

Figure S6 Powder-XRD patterns of $CsPb_2Br_5$ SCs with different annealing temperatures for 24 hours.

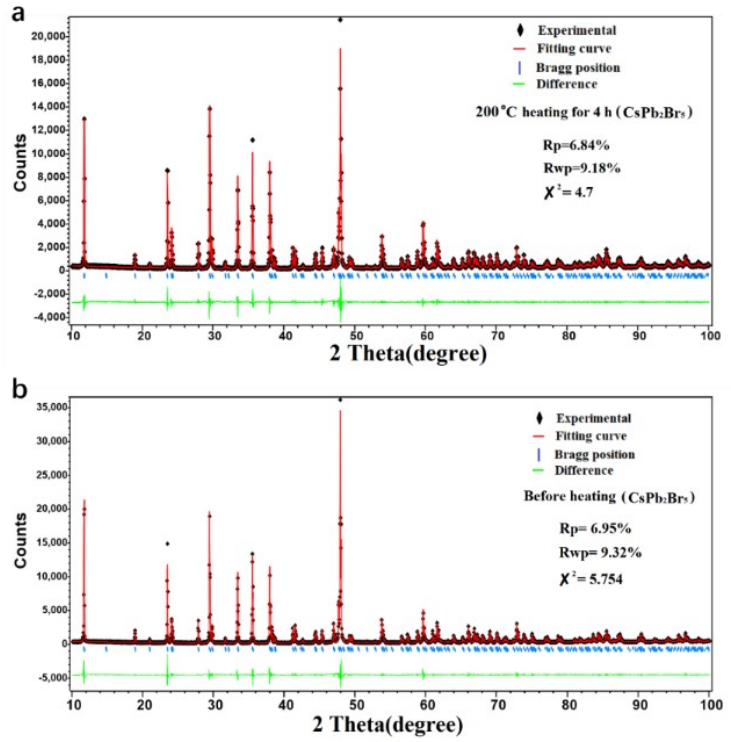

Figure S7 (**a, b**) Rietveld refinement pattern of powder XRD data for $CsPb_2Br_5$ SCs before (**a**) and after (**b**) thermal annealing.

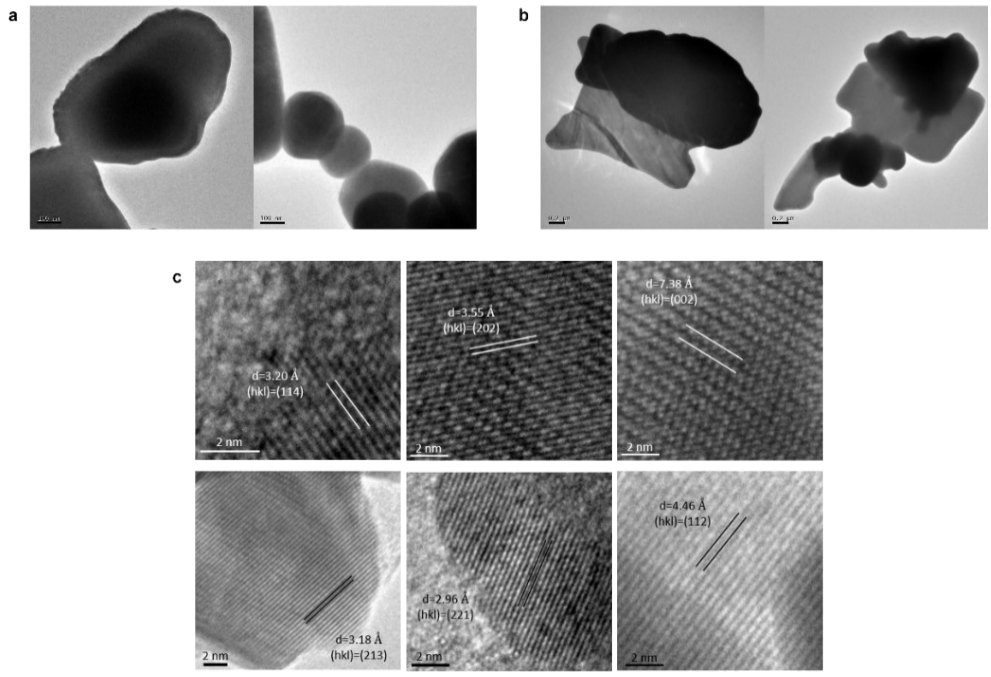

Figure S8 TEM (**a, b**) and HRTEM (**c**) images of $CsPb_2Br_5$ SC-powder before (**a**) and after (**b, c**) thermal annealing treatment.

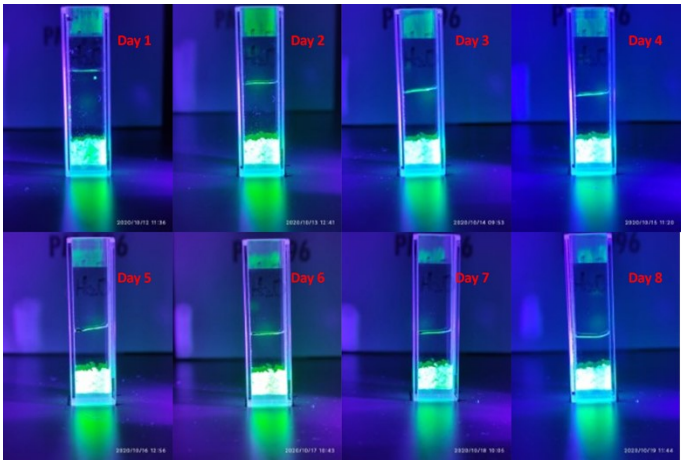

Figure S9 Photograph of the annealed $CsPb_2Br_5$ SCs immersed in water for 8 days under UV light illumination.

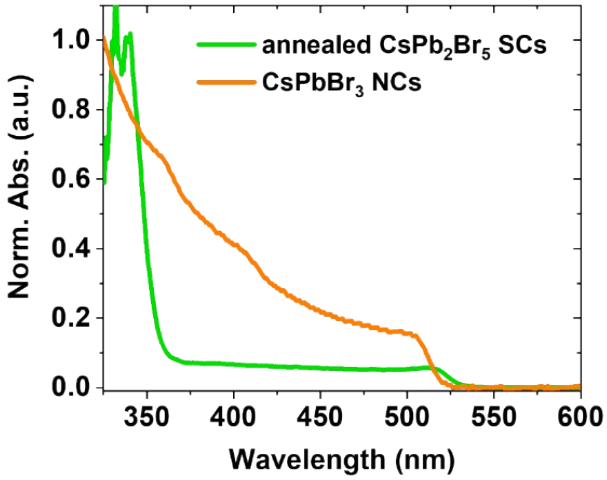

Figure S10 Absorption spectra of the annealed $CsPb_2Br_5$ SCs and pure $CsPbBr_3$ NCs.

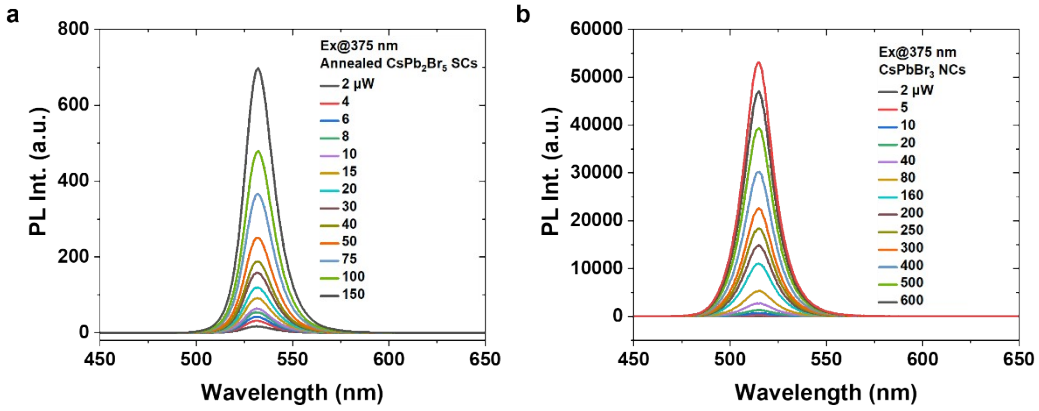

Figure S11 Excitation power dependent PL spectra of the annealed $CsPb_2Br_5$ SCs (**a**) and pure $CsPbBr_3$ NCs (**b**).

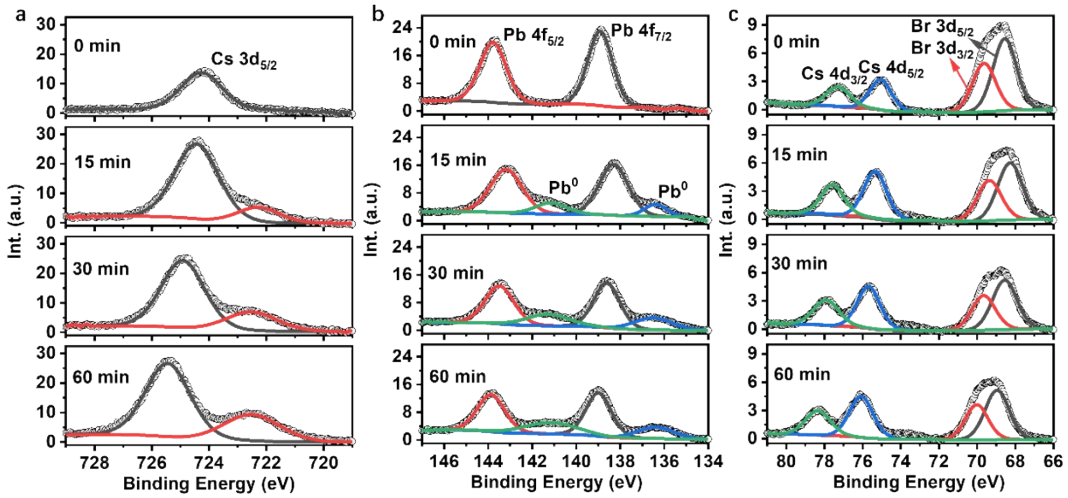

Figure S12 *In-situ* XPS spectra of $CsPb_2Br_5$ SCs during thermal annealing.

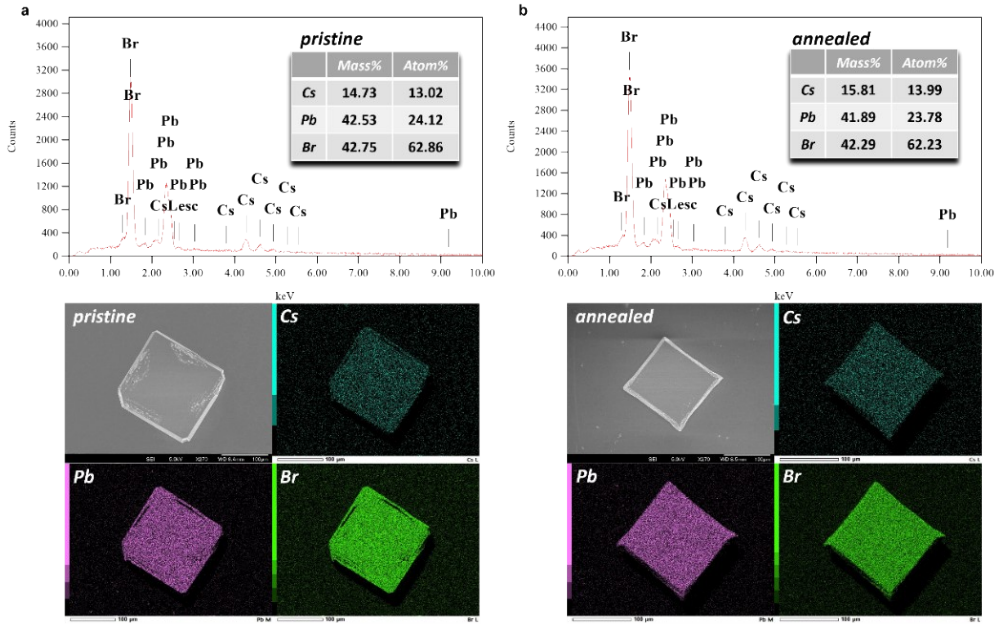

Figure S13 SEM-EDS spectra and mapping of the pristine (**a**) and annealed (**b**) $CsPb_2Br_5$ SCs (200°C, 4 h).

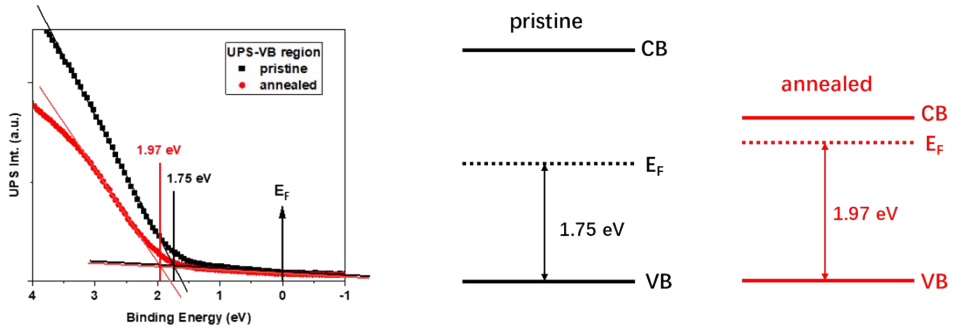

Figure S14 UPS spectra of the pristine and annealed $CsPb_2Br_5$ (200 °C, 1 hr). Position of valence band (VB) edges are marked with vertical bars (black for the pristine sample and red for the annealed sample), and Fermi level (E_F) is marked with a vertical arrow.

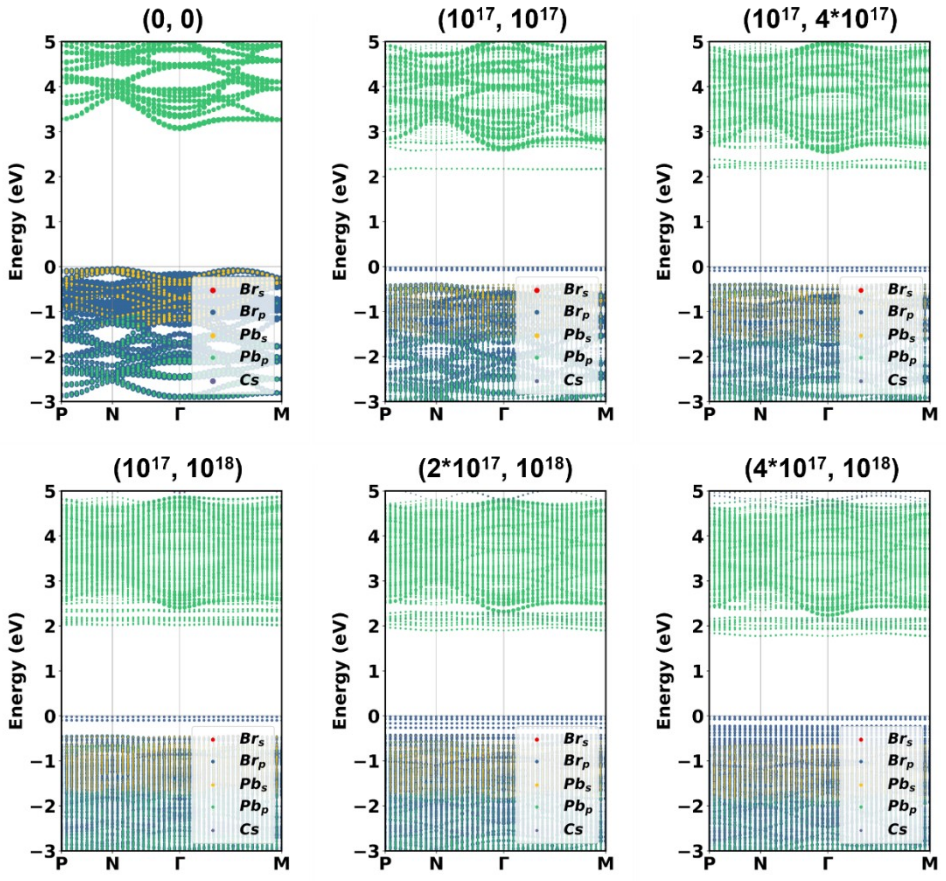

Figure S15 Band structures of $CsPb_2Br_5$ with different defect concentrations. Defect concentrations of (Cs_{Pb}, V_{Br}) are marked on the top of each panel in cm^{-3}.

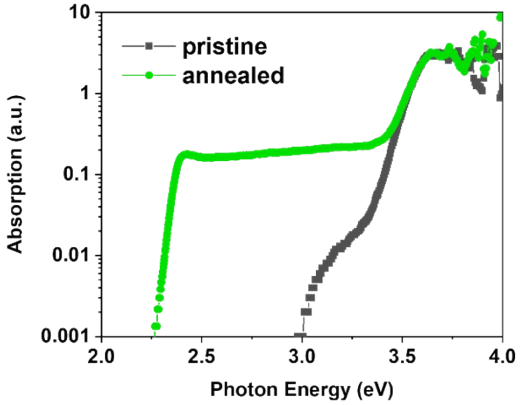

Figure S16 Absorption spectra of the pristine and annealed (150 °C, 8 hrs) $CsPb_2Br_5$ SCs. The data are the same as in Fig. 1d with the y-axis plotted in logarithms for a clearer comparison. A dramatic increase of the absorption near the band edge with a factor of more than 200 within 0.1 eV photon energy for the annealed $CsPb_2Br_5$. In contrast, the absorbance near the band edge of the pristine $CsPb_2Br_5$ increases by a factor of only 30 within 0.4 eV. Such dramatic increase in the absorbance slope near the band edge suggests a transition from indirect to direct bandgap after thermal annealing as the absorbance (A) near band edge for direct and indirect bandgap semiconductors has very different formula (ref. 65 and 66).

Direct bandgap: $A \propto A^{'} * \sqrt{h\nu - E_g}$, where A' is a certain frequency-independent constant, hν is photon energy, and Eg is bandgap.

Indirect bandgap: $$A \propto \frac{(h\nu - E_g + E_p)^2}{exp\left(\frac{E_p}{kT}\right) - 1} + \frac{(h\nu - E_g - E_p)^2}{1 - exp\left(-\frac{E_p}{kT}\right)}$$, where E_p is phonon energy, k is Boltzmann's constant, and T is temperature.

Direct bandgap semiconductors show a dramatic increase in absorbance when photon energy is just above the bandgap. In contrast, the absorbance near the band edge increases slowly with photon energy for indirect bandgap semiconductors, followed by a speedy increase due to photon energy being higher enough to allow direct optical absorption.

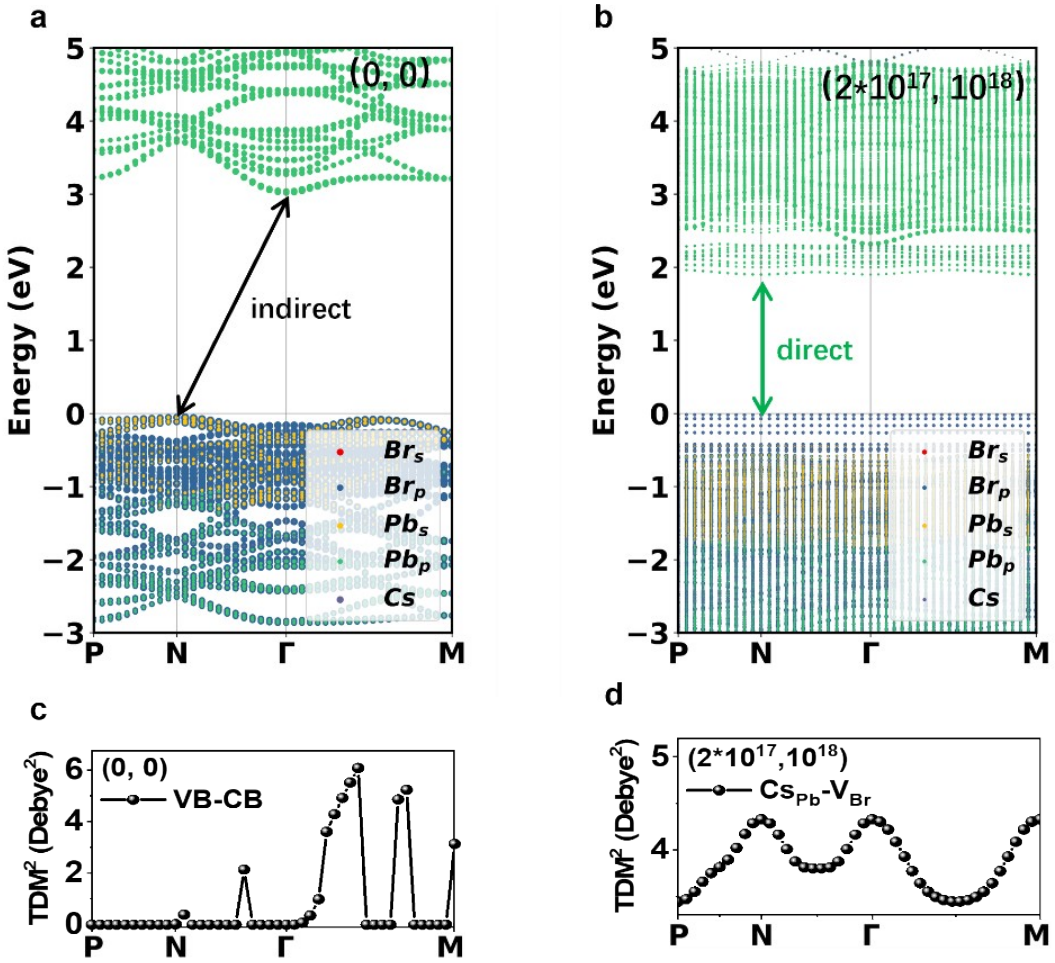

Figure S17 (**a-d**) Band structure and TMD^2 of $CsPb_2Br_5$ without defects (**a, c**) and $CsPb_2Br_5$ with defect concentration of ($2*10^{17}$,10^{18}) (**b, d**).

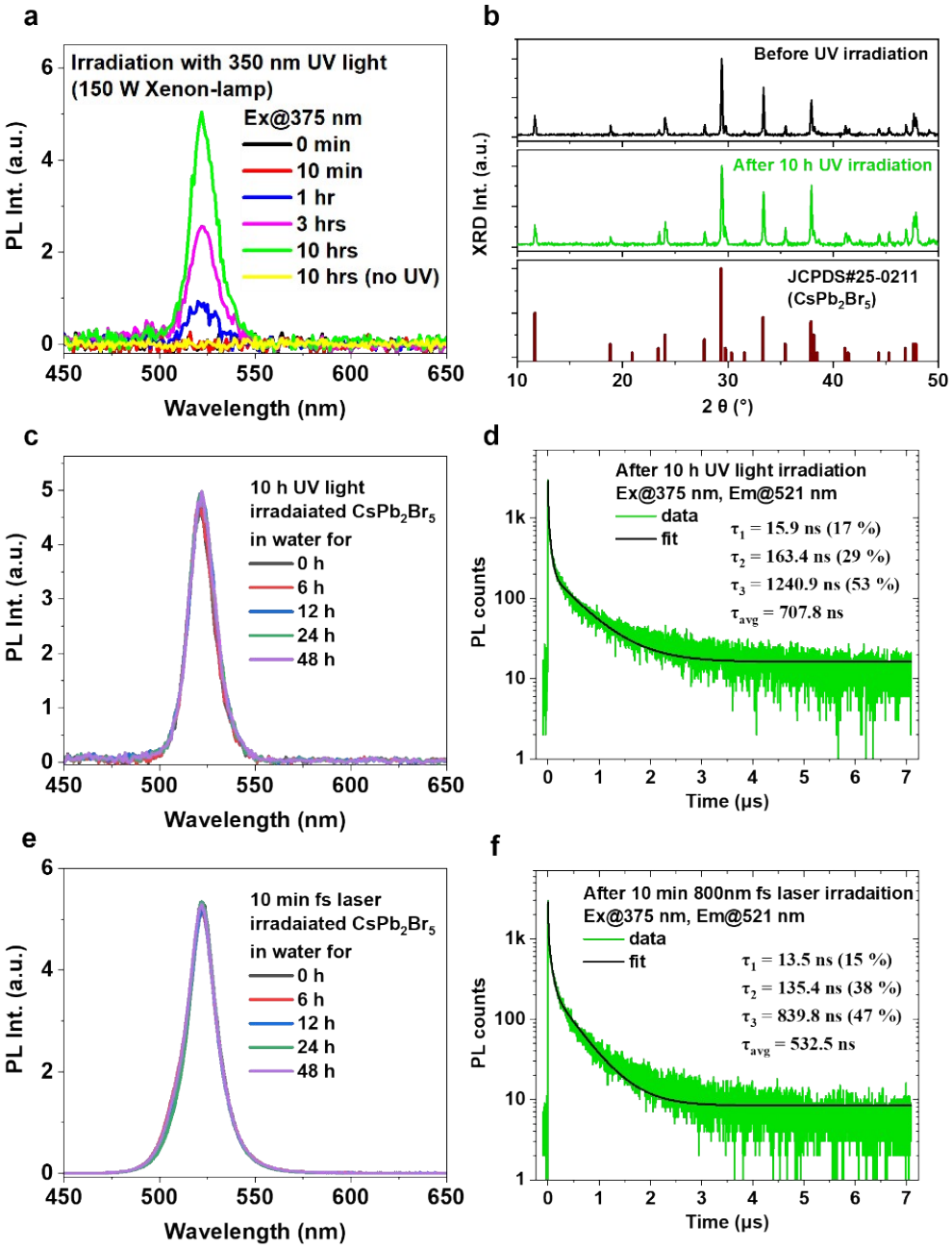

Figure S18 (**a**) Photoluminescence evolution of $CsPb_2Br_5$ SCs under 350 nm UV light irradiation; (**b**) powder-XRD of pristine and UV-light irradiated $CsPb_2Br_5$ SCs; Water stability measurements for (**c**) UV light irradiated and (**e**) fs-laser irradiated $CsPb_2Br_5$ SCs; Time-resolved PL measurements for (**d**) UV light irradiated and (**f**) fs-laser irradiated $CsPb_2Br_5$ SCs.

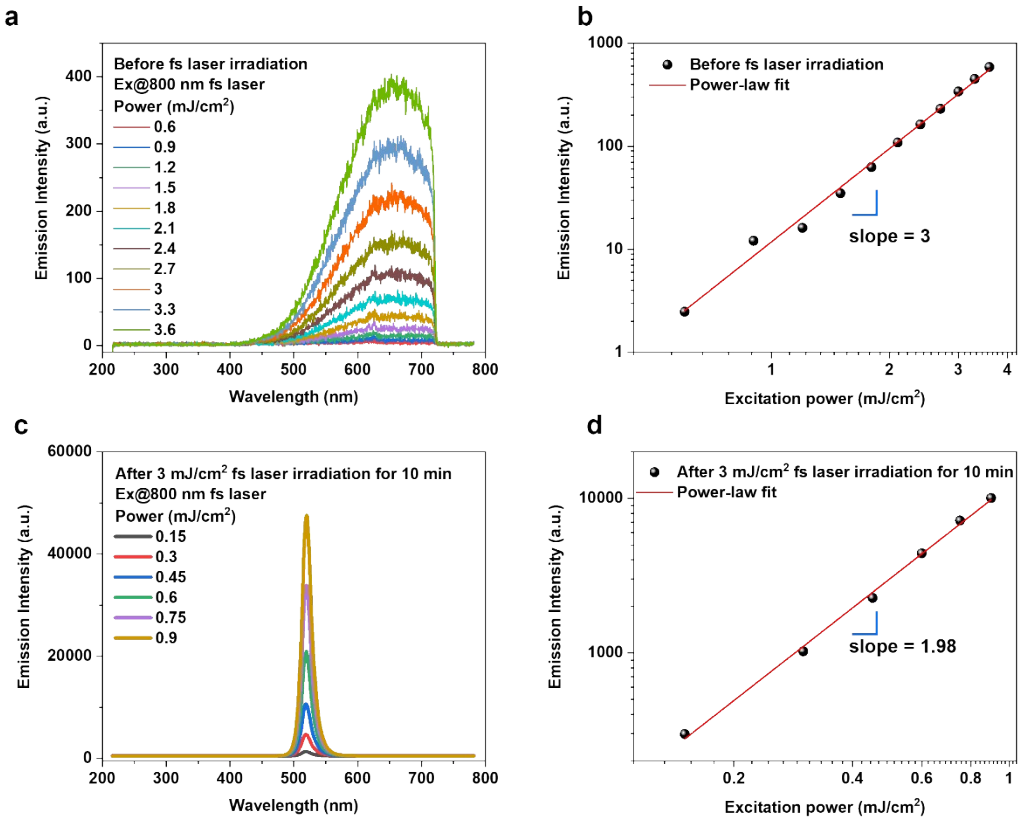

Figure S19 Excitation power-dependent emission spectra (**a, c**) and intensities (**b, d**) of $CsPb_2Br_5$ SCs before **(a, b)** and after **(c, d)** fs laser irradiation for 10 min (800 nm, 3mJ/cm^2). The excitation source for the emission spectra is 800 nm fs laser pulses.